J Electr Eng Technol Vol. 9, No. 3: 942-949, 2014
http://dx.doi.org/10.5370/JEET.2014.9.3.942

ISSN(Print) 1975-0102
ISSN(Online) 2093-7423

Low Cost Design Study of Brushless DC Motor for Electric Water Pump Application

Tae-Uk Jung†

Abstract – We studied about the rotor design change using a Ferrite ring magnet to reduce material cost in the condition of the same stator core design. However, this design direction has many weak points such as the decrease of BEMF, the low maximum output, the irreversible demagnetization characteristics of a permanent magnet and so on. In order to mitigate such disadvantages, an optimization design of the BLDC motor has been developed by changing each design parameter and by improving the electromagnetic structure. In the proposed water pump SPM BLDC motor using Ferrite magnet, the outer and inner diameter of stator is fixed to the value of the conventional IPM BLDC motor using Nd-Fe-B magnet. The design specification requirements should be satisfied with the same output power and efficiency characteristics in the same dimension. As a result of this study, the design comparison results considering driving performances and material cost are represented. Through the actual experiment with the prototype of the designed motor, the simulations results are verified.

Keywords: BLDC (Brushless DC) motor, Low cost design, Water pump, Rare-earth, Ferrite

1. Introduction

Recently, the research of permanent magnet brushless DC motors has been remarkably expanded because of the performance improvements by the use of rare-earth permanent magnets. And, the BLDC motor using the rare-earth has higher efficiency for energy saving, better performance with smaller volume and lighter weight, and it has a high power density.

The export regulation policies of the government of China, where at least 90% of the rare-earth materials are produced, have led to a price increase and an unbalanced supply of rare-earth materials [1]. Fig. 1 shows domestic rare metals price in china. At this moment when the cost of rare-earth permanent magnets is increasing, the research related to a motor design which reduces the amount of the required rare-earth permanent magnetic material to be used is attracting attention [2, 3].

In this study, a BLDC motor for a pump, in which the neodymium magnet is replaced with the Ferrite magnet, has been developed to cope with the cost increase and to ensure the stability of the resource supply.

One of the pump motors is an IPM rotor type BLDC motor using the neodymium. However, the motors using neodymium magnets should have large air-gaps. This is because the composition of neodymium magnet is based on metal materials so the motors using this magnet should have larger air-gaps and waterproofing for rust. On the other hand, other motors using Ferrite magnets are able to have enough effective air-gaps because Ferrite magnet is not based on metal materials so the rotor using this magnet does not need to be waterproof. This point means that Ferrite type motors are able to utilize effectively the rotor flux by having enough effective air-gaps.

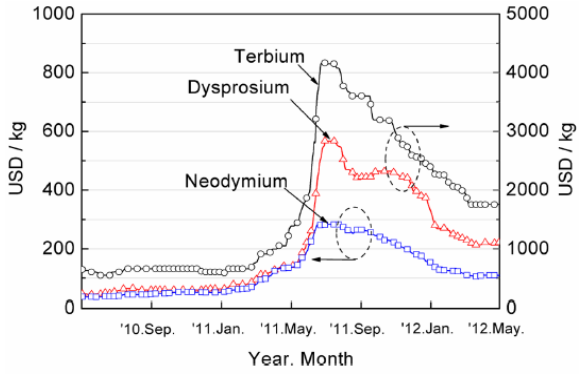

Fig. 1 Rare metals price trend in china

The use of Ferrite magnet causes deterioration in the performance of the motor. This causes the decrease in the back-electromotive force (BEMF), the maximum power of the motor and the irreversible demagnetization characteristic of the magnet. In order to compensate for the lower performance, the SPM type structure is adopted. This paper presents the low cost design technology using optimal parameters and electromagnetic structure.

2. Initial Design

2.1 Conventional BLDC motor for pump

The conventional BLDC motor for water pumps is the

† Corresponding Author: Dept. of Electrical Engineering, Kyungnam University, Korea. (tujung@kyungnam.ac.kr)
Received: January 28, 2013; Accepted: March 14, 2014

20[W] IPM motor using the neodymium magnet. The detailed design specifications and the photographs are represented in Table 1 and Fig. 2. The concentrated windings are wound on 9 slots and the salient structural 6 poles with Nd-Fe-B magnet are in the IPM type rotor.

In this water pump structure, water can be leaked into inner part which rotor is placed. The urethane molding waterproof insulation is applied to prevent the rust of Nd-Fe-B magnet in the rotor.

Therefore, the air gap length would be increased by the thickness of waterproof insulation. It causes the increase of magnetic resistance of air gap flowing flux. Therefore, the Nd-Fe-B magnet having high residual flux density is applied in the conventional water pump motor. Even though the material cost of rare earth Nd-Fe-B magnet is the great part of total material cost, the flux utilization of magnet is not efficient due to the long air-gap length.

The proposed rotor structure is focused on this issue. The ferrite magnet instead of the rare earth magnet is applied to minimize the material cost of magnet. And the rotor structure is redesigned using ferrite magnet with the same stator core structure.

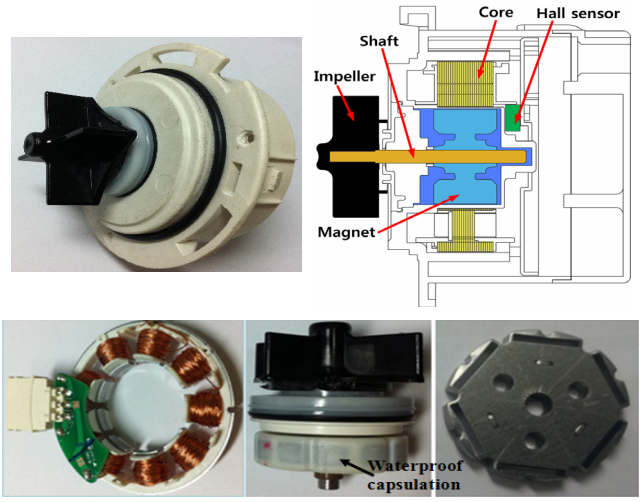

Fig. 2. Conventional IPM BLDC motor for water pump using Nd-Fe-B magnet

Table 1. Specifications of conventional water pump

Part	Item	Value
Rated Spec.	Rated Speed [rpm]	3600
	Rated current [A]	1.52
	Rated Torque [rpm]	0.054
	Rated Output [W]	20
Stator	Outer Dia. [mm]	58.07
	Inner Dia. [mm]	30.4
	Stack length [mm]	5
Rotor	Outer Dia. [mm]	27.4
	Stack length [mm]	5
Air gap [mm]		1.5
Turns		128
Winding connection type		Y connected
Pole / Slot / Winding		6 / 9 / Concentrated
Permanent magnet		NdFeB38

2.2 Magnetic equivalent of SPM BLDC motor

The equivalent magnetic circuit is configured to obtain the air-gap magnetic flux density of the permanent magnet motors, and the permeability of the core is assumed to be infinite for the convenience of the analysis. Fig. 3 shows the magnetic path. From the Eq. (1), the magnet flux is shown as divided into the leakage flux and the effective air-gap flux [6, 7].

The leakage coefficient f_{lkg} is defined as the ratio of air-gap flux to magnet flux as:

$$f_{lkg} = \frac{\phi_g}{\phi_M} = \frac{\phi_g}{\phi_g + \phi_l} \tag{1}$$

Where, φ_g is the effective air-gap flux, φ_l is the leakage flux, φ_M is the magnet flux. The leakage coefficient is less than 1, and its value depends on the configuration of the motor.

Fig. 4 shows the magnetic equivalent circuit of one pole. The leakage permeance P_L is in parallel with the magnet internal permeance P_M. The armature MMF F_a due to phase current is shown as an MMF in series with the air-gap reluctance R_g, but it will be assumed initially that F_a = 0 (open-circuit conditions) [6].

2.3 Analysis modeling

The governing differential equations describing the dynamic behavior of single-phase BLDC fan motor can be described as:

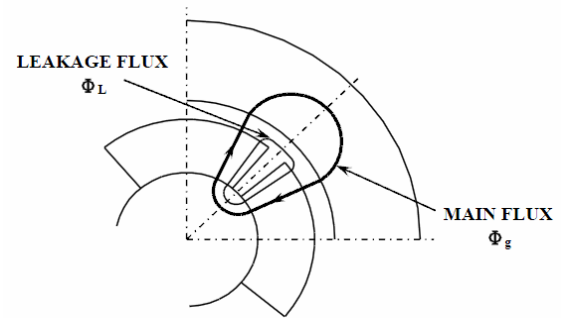

Fig. 3. Main flux path in surface-magnet motor

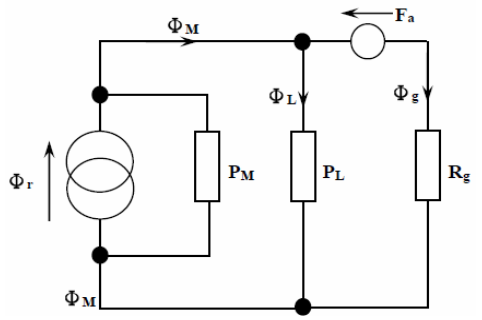

Fig. 4. Magnetic equivalent circuit of one pole

$$V_a = L_s \frac{di}{dt} + iR_s + V_{emf} \quad (2)$$

Where, V_a is the phase voltage input, R_s and L_s are the series resistance and the series inductance of stator winding, respectively, V_{emf} is the back-EMF induced by rotor flux variation. The torque-speed characteristics can be formulated as:

$$T_e = J_m \frac{d\omega}{dt} + B_m\omega + T_L \quad (3)$$

Where, T_e is the developed electromagnetic torque, J_m is the moment inertia, B_m is the viscous frictional coefficient and T_L is the load torque. The above Eqs. (2) and (3) are similar to two ordinary differential equations of brush dc motor. The energy transforms from electrical system to mechanical system is based on

$$V_{emf} = K \cdot \phi_f(\theta) \cdot \omega = K_e \cdot \omega \quad (4)$$

$$T_e = K \cdot \phi_f(\theta) \cdot I = K_t \cdot I \quad (5)$$

Where, K is the constant, φ_f is the value of normalized flux distribution. The torque constant K_t is equivalent to the back-EMF constant K_e. In this application, however, K_t and K_e are function of rotor position because of flux distribution. It means that the back-EMF voltage varies with rotor position. For this reason, building up the table in term of flux distribution is necessary to confirm accuracy of the equivalent model.

2.4 Design procedure of BLDC motor

The proposed motor is the SPM BLDC motor using Ferrite magnet. Unlike in the IPM motor, the reluctance torque is not generated and only the magnetic torque is generated because of not having air-gap length changes. The aim of the present study is to design the SPM rotor in which the rare-earth magnet is replaced with the Ferrite magnet. The design for the stator shape in the proposed BLDC motor is carried out under the same conditions with the conventional BLDC motor.

Table (2) shows the comparison of the characteristics between the Ferrite magnet used in the proposed motor and the Nd-Fe-B magnet used in the conventional motor [6]. As the characteristics of the core, a non-oriented silicon steel sheet is used. The design procedure of the proposed motor is performed through the flow chart shown in Fig. 5. Fig. 6 shows the modeling of the conventional IPM motor and the proposed SPM motor, and they are analyzed by FEA.

2.5 Design of thickness of ferrite magnet

The Ferrite thickness is designed to have safe in demagnetization for withstanding the magnetic field generated from the maximum current in the stator winding.

The safety condition for demagnetization is $U_m + F_m \leq H_m \cdot l_m$, wherein the bend(curve, line) point of the demagnetization is H_m, and the magneto-motive force of the rotor surface by the stator current is F_m.

The thickness of the neodymium magnet in the

Table 2. Property of material used for BLDC motor

Employed material		
Magnet	Neodymium	NdFeB38H
		Br : 1.21 ~ 1.25 [T]
		-Hc : ≥ 899 [kA/m]
	Ferrite	NMF-7BE
		Br : 0.41~0.43 [T]
		-Hc : 286~326 [kA/m]
Steel sheet		50A1300(S60)
		Non-oriented silicon steel sheet
		Density : 7.9 [g/cm^2]
		Sheet thickness 0.5 mm

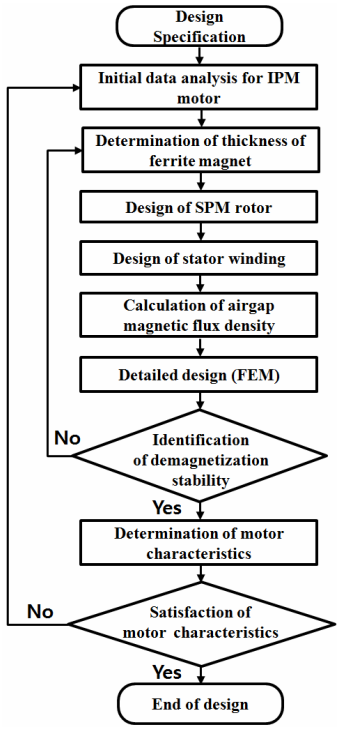

Fig. 5. Flow chart for design of proposed BLDC motor

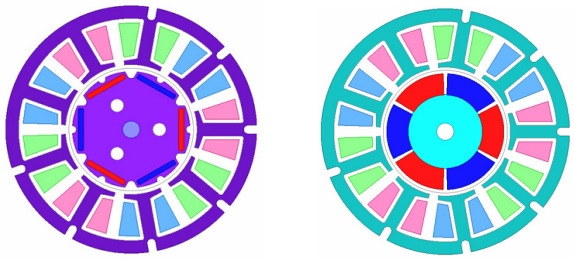

(a) Conventional model (b) Proposed model

Fig. 6. 2D FEA modeling of BLDC motor

conventional motor is 1.2 [mm], and the demagnetization current is 14 [A]. The thickness in the case of Ferrite is 3.5 [mm]. Also, the final determination of the thickness should be made by the BEMF and the output characteristics.

3. Optimization of the Proposed BLDC Motor

3.1 Design of Experiment (DOE)

The design of the proposed SPM motor is optimized by using the Design of Experiment (DOE).

Since the Ferrite magnet has weaker magnetic force than the neodymium magnet, the proposed motor should have narrow air-gaps. Therefore, the air-gap is designed as 1 [mm] through the capsulation removal.

Table 3 lists the mainly design parameters. Each parameter is divided into four levels. Fig. 8 shows the objective functions on the BEMF, the output torque, and the efficiency.

According to the DOE result, the stack length is the most influential factor in the output characteristic. Also, the number of turns is determined as 135 to keep the performance of the conventional motor.

Fig. 9 shows the estimated values of the factors plotted in a 3D space according to each level on 135 turn. Based on the selected design parameters, a RSM (Response Surface Method) is carried out. A response surface is the relationship between an objective function and design parameters. First, an appropriate analysis model for the response surface is assumed, and the data is obtained by performing experiments in various conditions of independent variables. Then, approximation function is estimated through a regression analysis. From the approximation function, a sensitivity analysis may be performed by analyzing changes of objective function according to the design parameters.

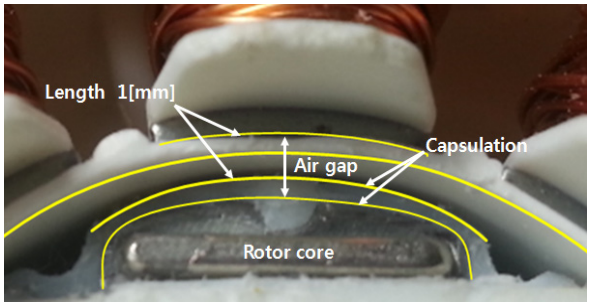

Fig. 7. Air-gap structure of the conventional BLDC

Table 3. Design parameters according to level

Design parameter \ Design level	1	2	3	4
Stack length [mm]	4	5	6	7
Thickness of magnet [mm]	3.5	4	4.5	5
Winding turns [turns]	125	130	135	140
Air-gap [mm]	1			

Lastly, the combination of design parameter to maximize the objective function is found and the results of this method are shown in Figs. 9 and Fig. 10 [8].

With these results of DOE, the stack length and the thickness of the permanent magnet are decided 6 [mm] and 5 [mm] respectively as the optimal conditions.

3.2 Design parameter of proposed BLDC motor

In order to meet the performance requirement of the

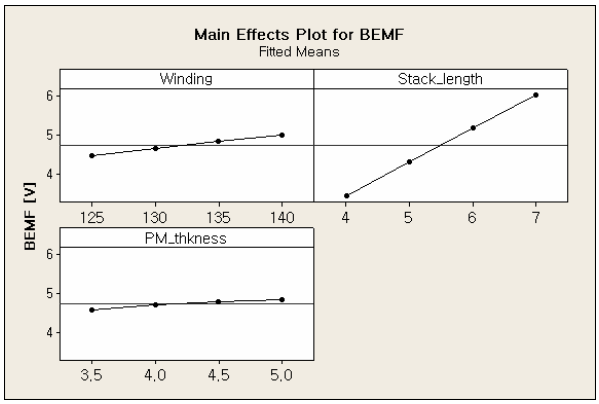

(a) Main effects plot for BEMF

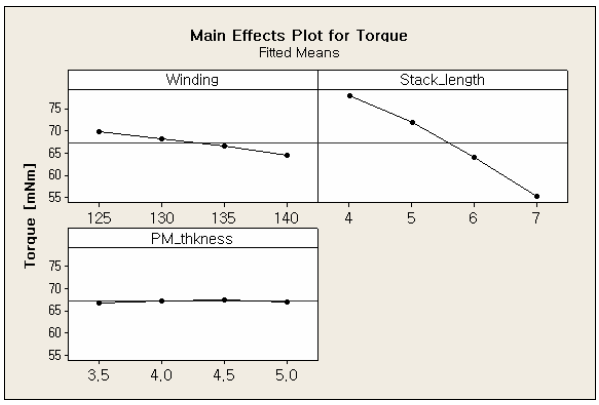

(b) Main effects plot for torque

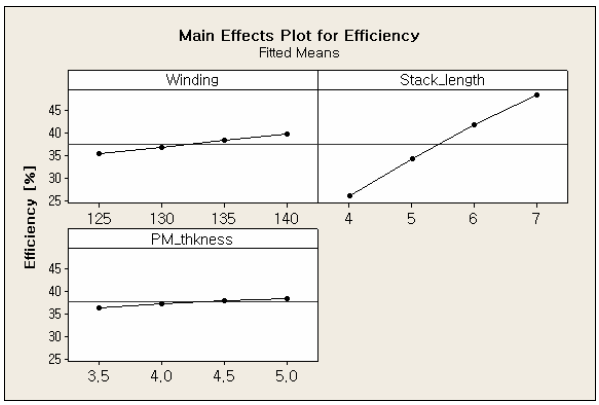

(c) Main effects plot for efficiency

Fig. 8. Analysis result of DOE

proposed motor, the accurate calculation of design parameter is important. The parameters K_e, the inductance, and the resistance are calculated by using the FEA. The design parameters of each motor are displayed in Table 4.

3.3 Characteristic of demagnetization

The demagnetization of a permanent magnet is definitely relevant to the temperature variance and armature reaction.

When the operating point of permanent magnet is passed through the knee point of demagnetization curve by the effects of temperature variance or armature reaction, the permanent magnet cannot be recovered to the original operating point because of the irreversible demagnetization.

Therefore, the demagnetization analysis of a permanent magnet must be performed in the design process [9, 10].

Fig. 11 shows the process of demagnetization analysis. The magnet thickness and shape can be optimized through this process.

With respect to the demagnetization characteristics of Ferrite, the maximum temperature is set to be 100℃ and

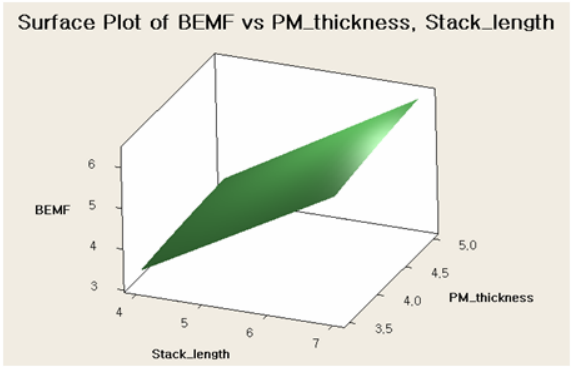

(a) RS of BEMF

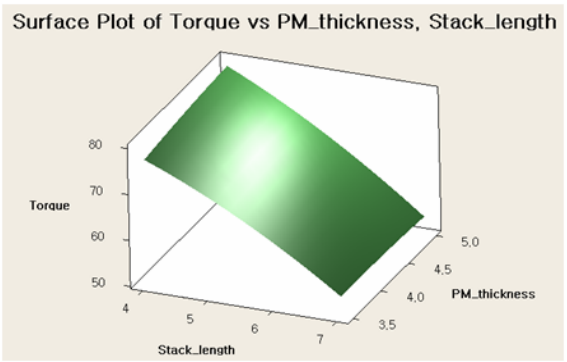

(b) RS of torque

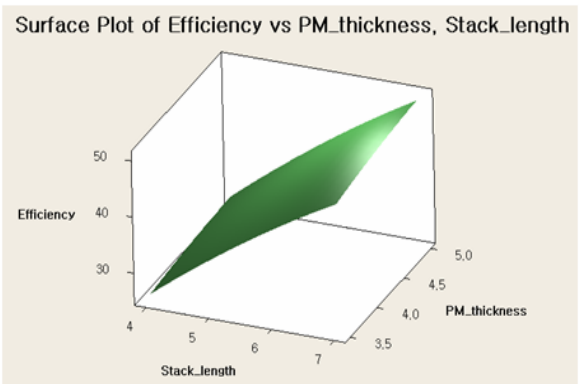

(c) RS of efficiency

Fig. 9. Result of Response Surface analysis (135 turn)

Table 4 Design parameter of BLDC motor

Item	Value	
	conventional	Proposed
Air-gap length [mm]	1.5	1
Stack length [mm]	5	6
Winding turns [turns]	128	135
Phase Resistor [Ω]	1.7	2.2
K_e (/ turn·ω_m)	0.00015	0.00015

FEAlysisf Taects plot for Eation

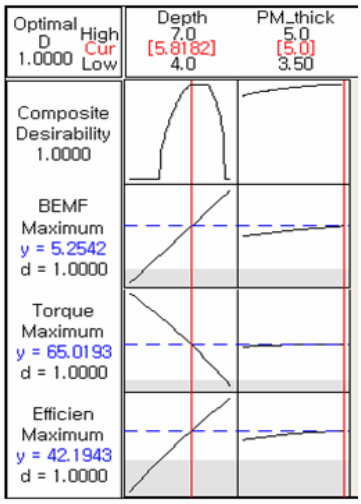

Fig. 10. Results of the response surface

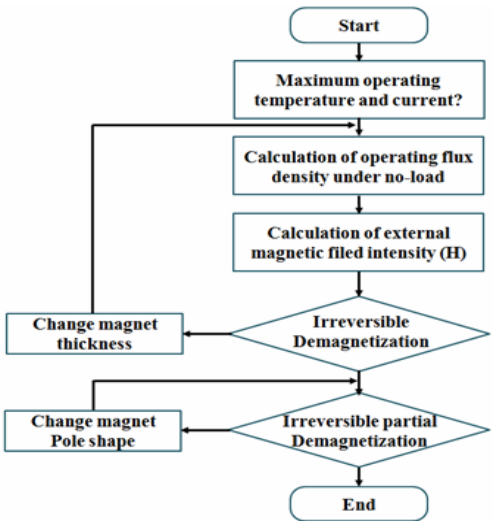

Fig. 11. Flow-chart for demagnetization analysis

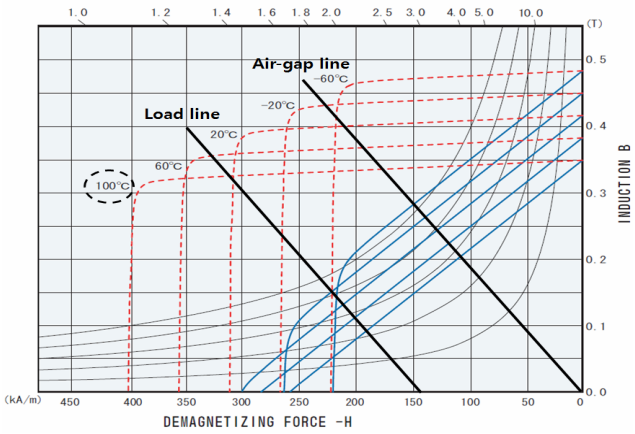

Fig. 12. Permanent magnet demagnetization analysis results

the maximum current is set to be 12 [A]. Fig. 12 is shown on the air-gap magnetic flux density calculated by the FEA upon being subject to a no-load condition. As to the external magnetic field generated by the stator current, the load line parallel to the air-gap line is indicated after the calculation. As the result, the load line is positioned on the safety point of the demagnetization curve line, and thus, what the irreversible demagnetization is not occurred is confirmed in the optimized design [10, 11].

4. Experiment for Characteristics of BLDC Motor

4.1 Characteristics of BEMF

Fig. 13 shows the prototype rotor of proposed motor. Due to the low magnetic flux density of Ferrite, the stack length and the number of turns considered with fill factor are increased to keep the BEMF level.

Both the motors are analyzed by the dynamometer system shown in Fig. 14. As shown Fig. 15, the peak BEMF level of the conventional motor is higher than the proposed one. However, the BEMF waveform of the optimized motor is nearly a sin waveform.

4.2 Load characteristics

In order to use the BLDC motor proposed in the present study, this motor should have the same output characteristic with the conventional BLDC motor. To confirm such characteristics, the measured output S-T curve characteristics of the proposed BLDC motor is compared with the IPM motor and the FEA result, as shown in Fig. 16.

The torque values of the conventional motor and the designed motor at the rated speed 3600 [rpm] are 0.06 [Nm] and 0.063 [Nm], respectively. And, the curve result requiring the same load characteristics of the conventional IPM BLDC motor is confirmed.

Also, the proposed BLDC motor has higher efficiency

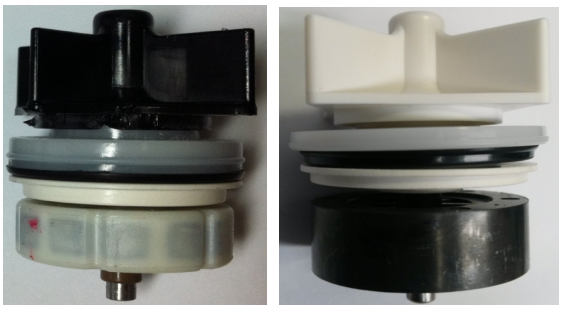

(a) Conventional rotor (b) Proposed rotor

Fig. 13. Comparison of rotor shape

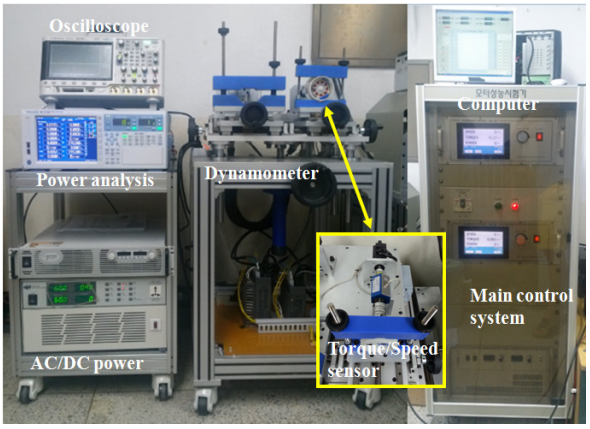

Fig. 14. Dynamometer system for experiment

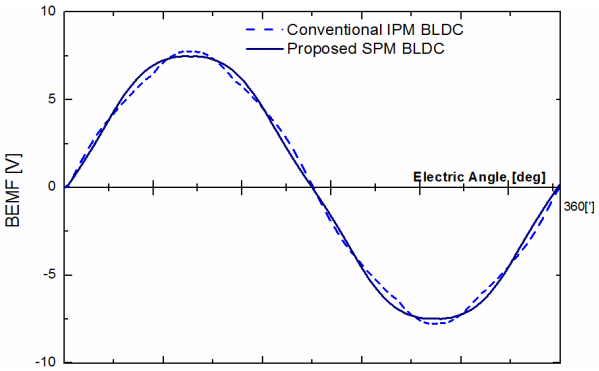

Fig. 15. Comparison of measurement results of BEMF

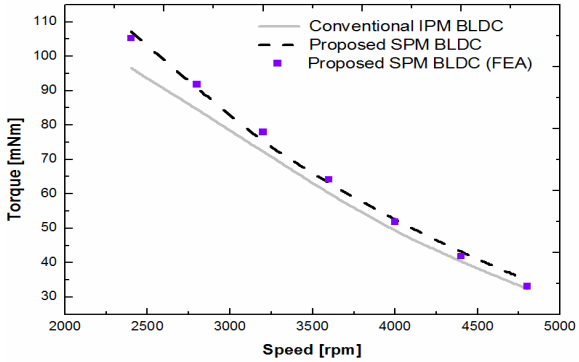

Fig. 16. Comparison of S-T curve characteristics

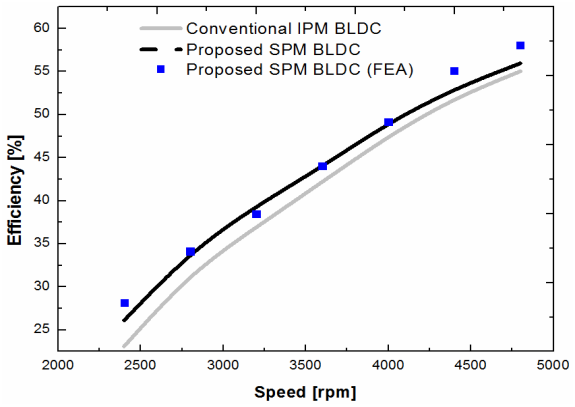

Fig. 17. Comparison of efficiency characteristics

Table 5. Comparison of output characteristics

Unit	Conventional IPM	Proposed SPM
Input DC Voltage [V]	12	
Speed [rpm]	3600	
Current [A]	1.52	1.34
Torque [mNm]	60	61.5
Output [W]	22.6	23
Efficiency [%]	42.1	42.8
Torque ripple [%]	12.2	9

Table 6. The comparison of material cost composition

Motor type	Items	Copper	Permanent magnet	Si-steel	Total cost (Won)
Conventional	Used weight (g)	27.8	3.8	27.8	1136.9
	Unit price (Won)	9.5	200.0 (Nd-Fe-B)	4.2	
	Cost (Won)	263.9	756	117	
	Cost rate (%)	23.2	66.5	10.3	100
Proposed	Used weight (g)	35.2	8.8	18.5	588.7
	Unit price (Won)	9.5	20.0 (Ferrite 9BE)	4.2	
	Cost (Won)	334.0	176.8	77.9	
	Cost rate (%)	56.7	30.0	13.2	100

than that of the conventional BLDC motor, as shown in Fig. 17. Table 5 shows the results for the performance specifications of the conventional motor and the proposed motor.

4.3 Material cost comparison

Table 6 shows the comparison for the main material costs and the composition rate.

The design result determines that the price of the proposed motor is more economical than that of the conventional BLDC motor using the Nd-Fe-B magnet. Although the used amount of coil is increased, the used amount of Si-steel core is decreased by approximately 35[%] because only the bonded ring type ferrite magnet is used without the core. Above all things, the cost of magnet is reduced 77[%] by changing of magnet material. Therefore, in the total cost, the proposed SPM motor using ferrite magnet has competitive price of 51.8[%] of conventional IPM motor using Nd-Fe-B magnet.

5. Conclusion

In this paper the cost reduction design is studied to release the cost burden of BLDC motor for electric water pump using Nd-Fe-B material magnet.

In order to minimize the material cost of permanent magnets, firstly, the magnet material is changed as ferrite magnet. By this, the air-gap length is largely reduced by the elimination of water proof capsulation of water pump. It helps the utilization of rotor magnet flux. And the appropriate design specification is decided by DOE and RSM applying FEA analysis.

As a result, the total material cost is decreased nearly 50[%] keeping the similar level of driving efficiency. The result of design change is approved by the experiment of prototypes.

Acknowledgement

This work was supported by Kyungnam University Foundation Grant, 2012.

References

[1] H. J. Kim, S. M. Kim, “Rare Earth Dispute and Trend in Development of NdFeB Anisotropic Bonded Magnets”, Journal of the Korean magnetics society, v. 22 no. 3, pp. 109-115, 2012.

[2] J. G. Lee, J. H. Yu, H. J. Kim and T. S. Jang, “Trend in Research and Development Related to Motors and Permanent Magnets for Solving Rare-earth Resources Problem”, Journal of the Korean Magnetics Society, Vol. 22, No. 2, April, 2012.

[3] Jung-Pil Yang, “The Current Status and Future Outlook of the Bonded Rare-earth Magnet”, Journal of the Korean Magnetics Society, Vol. 21, No. 4, August 2011.

[4] Jung-Goo Lee, Youn-Kyoung Baek, Ji-Hun Yu and Chul-Jin Choi, “Trend in Research and Development Related to Lean Heavy Rare-earth Permanent Magnets for Next-generation Motors”, J. Kor. Powd. Met. Inst., Vol. 19, No. 2, 2012.

[5] Su-Jin Lee, Sung-Il Kim, Jung-Pyo Hong, Byoung-Young Song, Jong Won Park, “Characteristic Analysis of the Water Pump Motor considering Polar Anisotropic Ferrite Bonded Magnet”, Electrical Machines and Systems(ICEMS), pp. 1242-1245, Oct. 2010.

[6] Byeong-woo Kim, Hyun-dock Cho, Do-hee Lee, "Characteristic Analysis of BLDC Motor for Vehicle Compressor Based on High Voltage", Transactions of Korean Society of Automotive Engineers, vol. 16 no. 3, pp. 44-51, 2008.
[7] Duane Hanselman, "Brushless Permanent Magnet Motor Design", The Writers' Collective, 2003.
[8] A. I Khyri, J. A. comell, Response Surfaces: Designs and Analyses. New York: marcel Dekker, 1996.
[9] S. Zeze, T. Todaka, and M. Enokizono, "Improvement of Rotor Structure of Concentrated Surface Permanent Magnet Synchronous Motor", Electrical Machines and Systems (ICEMS), pp. 1-6, Nov., 2009.
[10] Jang-Young Choi, Hyung-Il Park, Seok-Myeong Jang and Sung-Ho Lee, "Design and Analysis of Surface-Mounted PM Motor of Compressor for Electric Vehicles Applications according to Slot/Pole Combinations", The Transactions of the Korean Institute of Electrical Engineers, vol. 60 no. 10, pp. 1846-1857, 2011.
[11] Masayuki Sanada, Yukinori Inoue and Shigeo Morimoto, "Rotor Structure for Reducing Demagnetization of Magnet in a PMASynRM with Ferrite Permanent Magnet and its Characteristics", Energy Conversion Congress and Exposition (ECCE), 2011 IEEE, pp. 4189-4194, Sept. 2011.

Tae-Uk Jung He received the B.S., M.S. and Ph.D. degrees in electrical engineering from Busan National University, Busan, Korea, in 1993, 1995 and 1999, respectively. Between 1996 and 2005, he was a Chief Research Engineer with Laboratory of LG Electronics, Korea. Between 2006 and 2007, he was a Senior Research Engineer of Korea institute of Industrial Technology, Korea. Since 2007, he has been with Kyungnam University as a Professor. His main research topic is concerning about the design and application of small wind turbine PM generator and BLDC motor drive system.